CHARACTERIZATION TESTING OF A 40 AMPERE HOUR BIPOLAR NICKEL–HYDROGEN BATTERY

JEFFREY C. BREWER*

NASA Marshall Space Flight Center, Huntsville, AL 35812 (U.S.A.)

MICHELLE A. MANZO and RUSSEL P. GEMEINER

NASA Lewis Research Center, Cleveland, OH 44135 (U.S.A.)

Summary

Extensive characterization testing has been done on a second 40 ampere hour (A h), 10-cell, bipolar nickel–hydrogen (Ni–H$_2$) battery to study the effects of operating parameters such as charge and discharge rates, temperature, and pressure on capacity, A h and watt hour (W h) efficiencies, end-of-charge (EOC), and mid-point discharge voltages. Testing to date has produced many interesting results, with the battery performing well throughout the test matrix except during the high-rate (5 C and 10 C) discharges, where poorer than expected results were observed. The exact cause of this poor performance is, as yet, unknown. Small scale 2 in. × 2 in. battery tests are to be used in studying this problem.

Low earth orbit (LEO) cycle life testing at a 40% depth of discharge (DOD) and 10 °C is scheduled to follow the characterization testing.

Introduction

Space power systems of the future are projected to require power levels that extend far beyond the current levels of demand. In order to meet these increasing needs, improvements must be made to current energy-producing systems, or new technologies must be developed. Over the past several years, LeRC has been actively engaged in the development of a bipolar configured Ni–H$_2$ battery. This battery system has the potential to meet some of these high-power needs of the future. In a continuing effort to develop this technology to a point where it can be used efficiently in space flight, LeRC has begun testing a second, 40 A h, 10-cell, bipolar Ni–H$_2$ battery.

Results from the tests on the first battery tested here at LeRC were very encouraging. The battery operated for some 10 000 LEO cycles at 40% DOD and produced promising results in most of a variety of characterization tests [1]. Following the completion of this test, work began on

---

*Author to whom correspondence should be addressed.

the design of the second bipolar battery in the hope of developing an improved battery.

Battery design

The basic design of this battery differs from that of the first battery only through slight modifications in the cell frames. Poor, high-rate discharge performance and electrolyte leakage paths in the first battery led to these changes. It was thought at the time that a possible cause of the poor high-rate performance in the first battery was limited gas access to the reaction sites on the negative electrode. Gas-access area was thus increased by modifying the cell frame in an attempt to alleviate this problem. The gaskets were also changed in the cell frame design in an effort to improve the seals and thus better contain the electrolyte within the cells. In addition to these minor design changes, most of the individual components of the second battery came from different manufacturers (Table 1).

TABLE 1

Component differences between battery 1 and battery 2

Component	Battery 1	Battery 2
Frame	Polysulfone — Old	ABS — New
Nickel electrode	Eagle Picher	Whittaker — Yardney
Hydrogen electrode	LSI	Giner
ERP	Ni foam — Brunswick	Ni felt — Nat'l Std
Gas screen	Exmet	Woven (Nat'l Std)
Separator	Asbestos	Asbestos
Electrolyte	31% KOH	26% KOH

The reasons vary as to why these component changes were made. The frame material, for instance, was changed from polysulfone to ABS (resins which are terpolymers of acrylonitrile, butadiene, and styrene) because of superior machining capabilities and mechanical stability of the material. The nickel electrode was changed simply because of availability. The other changes were based, at least in part, on more technical reasoning and on the desire to reduce the number of parts. Because of inconsistencies found in the previous H_2 electrode, Giner, Inc. was engaged in a development program to manufacture a suitable large area, single unit electrode for this application. In doing so, the previous three-piece electrode would be eliminated. A program was also undertaken with National Standard to develop a fibrex electrolyte reservoir plate (ERP) which would contain pores in the desired range and could be manufactured in one piece. The previous ERP was constructed from nickel foam from Brunswick which, due to the large area required and manufacturing limitations, resulted in a six-piece

ERP. In an attempt to increase the effective current-carrying area between the gas screen and the bipolar plate, and to improve high rate performance, the gas screen was changed to a heavier, woven screen, as opposed to an expanded metal (Exmet) screen in the first battery. This change also created a large weight increase which makes it difficult to justify its use without major performance improvements. Finally, the electrolyte concentration was changed from 31% to 26% potassium hydroxide. This was done because of superior life seen in IPV Ni–H_2 testing [2]. These multiple component changes, as well as different testing procedures and unique cell characteristics, make it difficult to compare results from the two batteries directly. Some comparisons, however, are valid and will be made.

One feature consistent with the first battery is that both utilized an active cooling process. This is accomplished by pumping a coolant through alternate bipolar plates (cooling plates) in the battery stack. This enables temperature readings to be controlled very consistently and accurately throughout the entire cell. This is one advantage over IPV technology. In an IPV cell, temperatures in the stack can run 7 °C hotter than the measured temperatures outside the cell [3].

Procedures

After construction was complete, the battery was placed in a boiler plate pressure vessel, which was designed to meet safety requirements. Each cell was instrumented with voltage leads to measure individual cell voltages, together with a thermocouple attached to the bipolar plate in the hydrogen cavity to measure internal cell temperature. Additional thermocouples were placed on the exterior of the stack to obtain additional temperature measurements. The pressure vessel was equipped with a pressure transducer for measuring the hydrogen pressure, an oxygen sensor, and a relative humidity indicator. A Modicon programmable controller was used to run the test. All instrumented points were scanned and digitized every 18 s by a Neff multiplexer and stored by a central computer system for subsequent processing. The data could then be processed and received in both tabular and graphical form for each cycle.

Following the setup and checkout of the test hardware and data collection system, initial cycles were run to determine battery capacity. An initial capacity of 40 A h was assumed. The capacity determination cycles basically consisted of a $C/2$ rate charge with a 5% overcharge, followed by a C rate discharge to a battery voltage of 7.0 V or a low cell voltage of 0.5 V. C is defined as the rate at which the battery's capacity will be depleted in one hour. The low cell voltage cut-off of 0.5 V was used in order to prevent any cell from going negative and thus generating hydrogen. A $C/4$ drain to these same cut-off points followed this to complete the total cycle. As the cycles continued, the C value was adjusted several times until a consistent capacity was recorded, which was 40 A h. While some of the formation cycles were

run at 20 °C and 200 psi, the baseline capacity determination cycles were run at 10 °C and 200 psi.

Characterization tests were then run at a variety of charge and discharge rates, temperatures, and pressures. A full set of tests was run at 10 °C and 200 psi at charge rates of $C/4$, $C/2$, and C, and discharge rates of $C/4$, $C/2$, C, 2 C, 5 C, 10 C, and 5 C pulse for each charge rate. Following this set of tests, subsets of this base characterization test were run at other temperatures and pressures. A $C/2$ rate charge was chosen as the charge rate to be used in these subsets. This selection was based, not only on performance in the base characterization test, but also on performance in prior tests [4]. A $C/2$ rate charge also allowed the cycles to fit better into an eight-hour day than if run at a lower rate. A subset of tests run at 20 °C and 200 psi consisted of the identical discharge rates used in the base set, paired with the $C/2$ charge rate. The remaining subsets (0 °C at 200 psi, 30 °C at 200 psi, and 20 °C at 400 psi) consisted only of the $C/4$, $C/2$, C, and 2 C rate discharges. Again, all were paired with the $C/2$ charge rate. Each individual test was run until three consistent cycles were recorded. Consistency was based on A h and W h efficiencies. Each cycle consisted of a full charge (the amount of which was equal to the capacity out in the preceding discharge plus a set percentage of overcharge) followed by a full discharge to a battery voltage of 7.0 V or a low cell voltage of 0.5 V (hereafter known as the normal cut-off points). A $C/4$ drain followed all discharges run at a $C/2$ rate or higher.

A set percentage of overcharge was used in this test in order to ensure adequate charging as well as protect from unnecessary overcharging. This is compared with the first battery test, where a set charge input was used for each cycle regardless of the capacity delivered in the previous discharge [1]. A 5% overcharge was used initially; however, this proved to be insufficient to recharge the battery adequately so the overcharge was increased to 10%. This percentage maintained a stable capacity from cycle to cycle; however, to reduce any unnecessary overcharging, the percentage was dropped to 7% where stable capacities were once again realized. The overcharge amount thus stayed at 7% throughout the remainder of the characterization testing.

Due to a lack of adequate manpower, cycles were not run over the weekends or holidays. This extended wet-stand period allowed time for a weak, high-resistance cell to self-discharge considerably more than the other cells. This delayed the resumption of the characterization testing until after that cell could be brought back up to a state of charge similar to that of the other cells. It was found through trial and error that the weak cell could be maintained by trickle charging the fully charged battery at a $C/150$ - $C/100$ rate. This method produced much more consistent results than other methods that were tried and allowed characterization cycles to resume much more quickly.

Results and discussion

Due to the wide range of variables in this test, all the relevant data will not be enumerated here, but are summarized in Tables 2 - 8.

Figures 1 - 4 contain pertinent voltage profiles from throughout the test.

Before discussion can begin on the specific test results, a general point needs to be made concerning the data to be discussed hereafter. The problems caused by a weak cell during extended wet-stand periods were mentioned earlier. This same weak cell also created problems during the characterization cycles. The discharges on most, if not all, of the early characterization cycles were terminated by a battery voltage of 7.0 V. This allowed good, accurate comparisons of data from cycle to cycle. The discharges on the vast majority of characterization cycles, however, were terminated by a low cell voltage of 0.5 V, while the overall battery voltage ranged from 7.1 to 10.4 V. Because most of the cycles thus had no common end-of-discharge (EOD) point, it was difficult to compare the basic, overall data between cycles. So, where it was helpful, capacity delivered to the 10.0 V point in the discharges was used to compare cycles in the hope of negating some of the distorting effects of the weak cell on the normal cut-off point data. Just what caused this cell to perform this way is still unknown, but it is thought that shunt currents could be present which allowed an additional discharge path through which the cell self-discharged overnight between cycles. This would explain the erratic behavior seen throughout the characterization cycles.

One additional comment about the data -- each data point represents the average value of the three most consistent cycles run at that particular set of test conditions.

Increasing the charge rate had little consistent effect on the capacity delivered to the normal cut-off points, although at lower charge rates the battery seemed to perform slightly better. Even the capacity delivered to 10.0 V showed no consistent trends (Table 2). Increasing the charge rate also had little consistent effect on the A h efficiency, but the accompanying

TABLE 2

Charge rate effects on capacities delivered to normal cut-off voltages and to 10.0 V at 10 °C and 200 psi
Battery EOD voltages shown under normal cut-off capacity values

Discharge rate	Capacity to normal cut-offs			Capacity to 10.0 V		
	Charge rate			Charge rate		
	$C/4$	$C/2$	C	$C/4$	$C/2$	C
$C/4$	47.45	46.90	46.87	43.15	42.85	43.06
	7.0	6.9	7.0			
$C/2$	46.80	46.12	43.72	42.60	42.02	40.34
	7.0	6.8	7.1			
C	41.73	42.38	40.84	37.75	39.08	38.97
	7.1	7.3	8.0			
$2C$	35.92	37.93	37.17	20.88	21.52	24.27
	7.1	7.1	7.4			

TABLE 3

Charge rate effects on A h and W h efficiencies at 10 °C and 200 psi

Discharge rate	A h efficiency (%)			W h efficiency (%)		
	Charge rate			Charge rate		
	$C/4$	$C/2$	C	$C/4$	$C/2$	C
$C/4$	94.16	93.60	93.77	80.16	78.17	74.45
$C/2$	87.76	86.30	85.95	72.43	69.21	66.20
C	76.99	77.04	75.76	60.43	58.93	55.83
$2C$	67.09	67.72	70.39	46.62	45.85	46.32

increase in battery charge voltage from an average of 15.52 V at the $C/4$ rate to 16.65 V at the C rate, caused an average decrease of 7.3% in the W h efficiency, except at the $2C$ rate discharge where no significant changes were seen (Table 3). Thus, because of its desirable effect on W h efficiency and lack of effect on other variables, a low charge rate would seem to be best; however, previous testing has suggested that a $C/2$ - C charge rate range should produce the optimum results [4]. It is difficult, however, to compare results from this characterization test directly with the reference test results due to the fact that the nickel electrodes used in both tests came from different manufacturers. The electrolyte concentration was also different. These differences alone could account for the discrepancies seen between the two tests. In each case, however, results failed to show strong proof that there is an optimum charge rate.

Increasing the discharge rate caused a consistent decrease in the capacity delivered over all temperatures and pressures except at 20 °C and 400 psi, where the capacity increased slightly from 46.03 A h to 47.46 A h at discharge rates of $C/4$ and $C/2$, respectively (Table 4). The probable cause of this apparent increase in capacity delivered at the higher rate can be traced to the weak cell causing an early termination of the discharges run at the lower rate. Comparing the capacities at the 10.0 V point in the discharge supports this theory. At 10.0 V, an average capacity of 43.99 A h was delivered at the $C/4$ rate and 42.59 A h was delivered at the $C/2$ rate.

Because of the lower capacities delivered at the higher discharge rates, the resulting A h efficiencies also decreased across the board (Table 5). Also, as discharge rates increased, W h efficiencies decreased over all temperatures and pressures due to the decrease in operating voltages that always accompany increasing discharge rates (Tables 6 & 7). In this report, operating voltages are reported as mid-point discharge voltages, which were calculated by averaging the following two data points: the voltage reading at 1/2 of the total discharge time and the voltage reading at the 20 A h out point. Discharge voltage profiles *versus* capacity at all discharge rates can be seen in Fig. 1.

TABLE 4

Capacity delivered to normal cut-off voltages at all tested conditions with a $C/2$ rate charge
Battery EOD voltages shown under capacity values

Discharge rate	Capacity (A h)					
	200 psi				20 °C	
	0 °C	10 °C	20 °C	30 °C	200 psi	400 psi
$C/4$	42.15	46.90	50.49	40.71	50.49	46.03
	9.7	6.9	7.4	7.9	7.4	8.9
$C/2$	41.19	46.12	47.68	37.50	47.68	47.46
	10.4	6.8	a	7.3	a	7.5
C	38.32	42.38	44.20	35.48	44.20	38.82
	9.3	7.3	7.3	9.2	7.3	8.7
$2\,C$	33.17	37.93	39.45	32.60	39.45	33.66
	7.6	7.1	7.2	10.3	7.2	9.0
$5\,C$	b	15.43	22.24	b	22.24	b
		7.0	6.9		6.9	
$5\,C$ pulse	b	30.60	33.97	b	33.97	b
		7.0	8.1		8.1	

aNo readings available due to data collection system errors.
b5 C and 5 C pulse run only at 10 °C and 20 °C at 200 psi.

TABLE 5

Ampere hour efficiencies at all tested conditions with a $C/2$ rate charge

Discharge rate	A h efficiency (%)					
	200 psi				20 °C	
	0 °C	10 °C	20 °C	30 °C	200 psi	400 psi
$C/4$	90.80	93.60	92.04	90.96	92.04	92.55
$C/2$	85.79	86.30	86.76	86.68	86.76	86.20
C	82.80	77.04	78.86	79.62	78.86	76.85
$2\,C$	72.67	67.72	72.39	72.23	72.39	68.38
$5\,C$	a	28.18	41.52	a	41.52	a
$5\,C$ pulse	a	52.08	65.18	a	65.18	a

a5 C and 5 C pulse run only at 10 °C and 20 °C at 200 psi.

The discharge rate effects were all as anticipated: at high discharge rates of 5 C and 10 C, however, performance was very poor. Poor performance was also seen at these rates in the first battery [1] but, despite attempts to alleviate this problem through design and individual component changes, even poorer performance was seen in the second battery (Fig. 2). In the attempts to run a 10 C discharge, the battery voltage dropped below 7.0 V within 30 s. Another 10 C discharge was run and was allowed to continue past the normal cut-off points down to a low cell voltage of 0.1 V.

TABLE 6

Watt hour efficiencies at all tested conditions with a $C/2$ rate charge

| Discharge rate | W h efficiency (%) | | | | | |
| | 200 psi | | | | 20 °C | |
	0 °C	10 °C	20 °C	30 °C	200 psi	400 psi
$C/4$	75.90	78.17	77.92	79.99	77.92	80.09
$C/2$	69.28	69.21	a	75.29	a	71.52
C	61.67	58.93	63.69	68.32	63.69	63.64
$2C$	46.51	45.85	53.43	41.26	53.43	52.91
$5C$	b	15.35	24.82	b	24.82	b

[a]No readings available due to data collection system errors.
[b]5 C and 5 C pulse run only at 10 °C and 20 °C at 200 psi.

TABLE 7

Mid-pt. discharge voltages at all tested conditions with a $C/2$ rate charge

| Discharge rate | Mid-pt. discharge voltage (V) | | | | | |
| | 200 psi | | | | 20 °C | |
	0 °C	10 °C	20 °C	30 °C	200 psi	400 psi
$C/4$	12.90	12.85	12.95	13.20	12.95	13.10
$C/2$	12.40	12.45	12.65	13.00	12.65	12.80
C	11.45	11.72	12.15	12.60	12.15	12.45
$2C$	9.70	10.15	11.10	11.83	11.10	11.55

This discharge lasted 3 min, but the voltage did not begin to level off until around 4.5 V (Fig. 1). The 5 C discharges lasted longer but again, failed to level off above a battery voltage of 7.0 V. (Tables 4 - 6 and Fig. 1). Only a 5 C pulse (1 s on/4 s off) discharge was able to produce meaningful results (Tables 4 and 5 and Figs. 1 and 3).

Several ideas have been discussed as to what could be causing this high-rate discharge problem. Limited gas access to the negative electrode was previously mentioned as a possible cause. The design changes mentioned earlier, that were made in an attempt to alleviate this problem, could, instead, have elevated the problem even more. This is based on the possibility that the holes drilled in the battery frame to allow gas access into the interior of the battery became filled with electrolyte and blocked free gas flow. One argument against this scenario is that the pressure of the gas flowing to, and from, the electrodes would keep the holes clear. Also, if gas access is the problem, then, based on the amount of H_2 located in the cavity adjacent to the negative electrode, initial voltage performance might
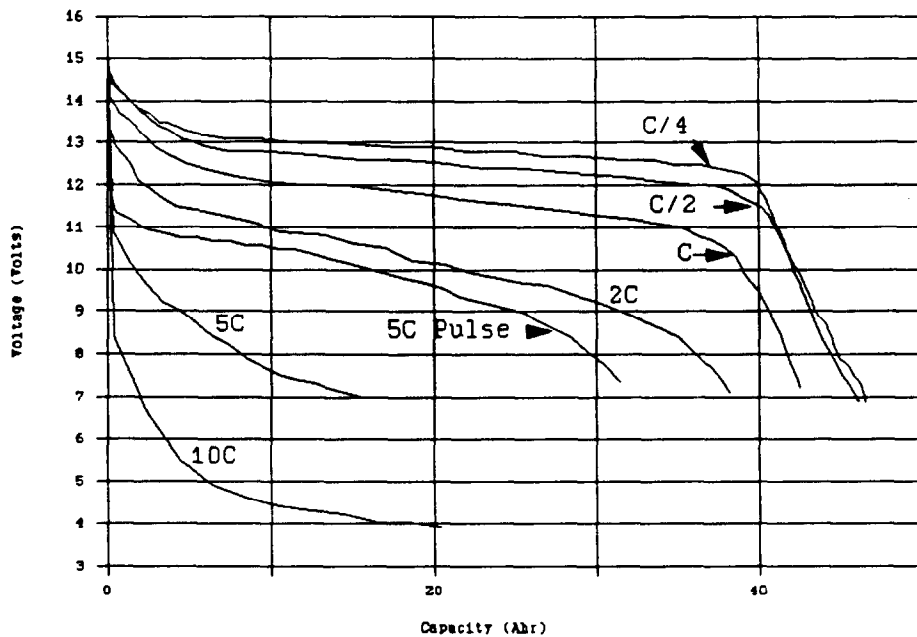
Fig. 1. Discharge voltage profiles *vs.* capacity for all discharge rates at 10 °C and 200 psi.
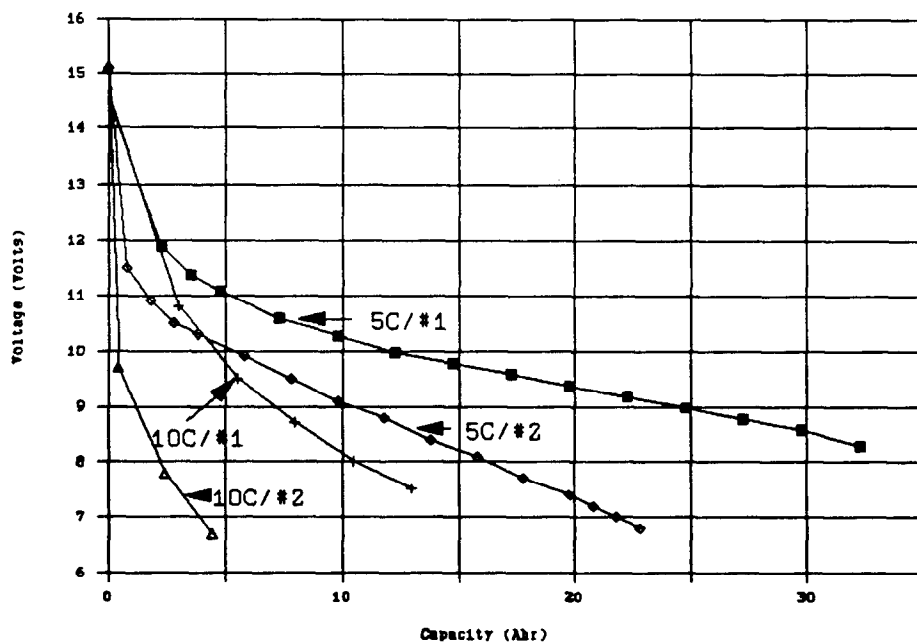

Fig. 2. 5 *C* and 10 *C* discharge voltage profile *vs.* capacity at 20 °C and 200 psi for battery 1 and battery 2.
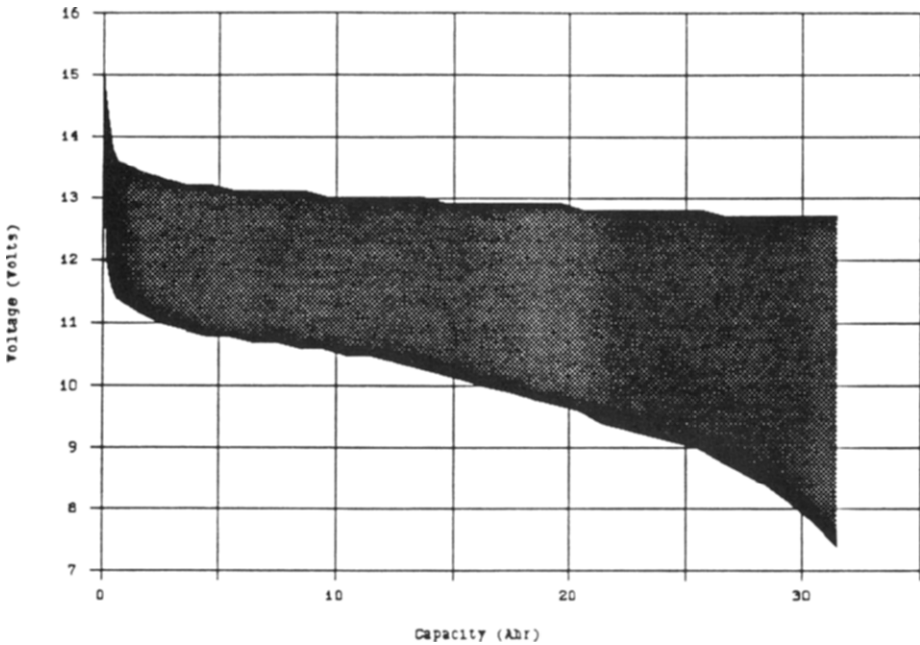
Fig. 3. 5 C pulse (1 s on/4 s off) discharge voltage profile *vs.* capacity at 10 °C and 200 psi.

be expected to be good but would fall off as the H_2 gas located in the cavity was used up. Data from the high-rate discharges showed no signs of good initial voltage performance and even showed signs of leveling off at a low voltage.

A second possible cause is poor contact between the gas screen and the two surrounding components — the negative electrode and the bipolar plate. Due to the large surface area of the bipolar stack components, uniform stack compression and the resulting surface contact between individual components is difficult to maintain consistently. A lack of adequate contact area would limit the current carrying capability and produce poor results, especially at high current levels.

Another possible cause is the Goretex backing placed on the H_2 electrode during the standard production process at Giner, Inc. Its presence could possibly be limiting the effective contact area between the H_2 electrode and the gas screen, thus hindering current flow. There was some initial concern about the possibility that this backing could cause current flow problems in a bipolar configuration, but polarizations of up to 500 mA cm^{-2} were operated successfully on a small scale prior to construction of the full size electrode. Perhaps the key point, once again, is the possible lack of uniform stack compression in a full scale battery configuration. One possible solution that has been discussed that could, at least, partially improve the contact between components is to weld the gas screen to the bipolar plate.

This would assure adequate contact area between these two components, but would not improve the contact area between the H_2 electrode and the gas screen. The effects on performance that the Goretex backing has in a full scale battery, as well as other possible problem areas, are to be addressed in further testing. Small scale 2 in. $\times$ 2 in. battery tests will begin soon and will be used to evaluate some of these areas.

Flooded capacity tests have already been done to evaluate the performance effects caused by varying the nickel electrode manufacturer and the electrolyte concentration. Electrodes from both manufacturers (Eagle Picher and Whittaker–Yardney) were tested at 10 C, 5 C, 2 C, C, $C/2$, and $C/4$ discharge rates using 26, 31, and 40% KOH as electrolyte. Nickel was used as the counter electrode and amalgamated zinc was used as the reference electrode. Results from this test showed no signs of inferior high-rate performance by the Whittaker–Yardney nickel electrode used in the second battery (Fig. 4). On the contrary, these electrodes produced much more stable efficiencies and capacities at all discharge rates tested (Table 8). The Whittaker–Yardney electrodes shown in Table 8 produced 76% of their low-rate ($C/4$) capacity at the high (10 C) rate, while the Eagle Picher electrodes delivered only 39% of their low-rate capacity at the high rate. It is not possible, however, to rule out completely the nickel electrode as being responsible for the poor high-rate discharge performance. Because of the flooded conditions under which these capacity measurements were made,
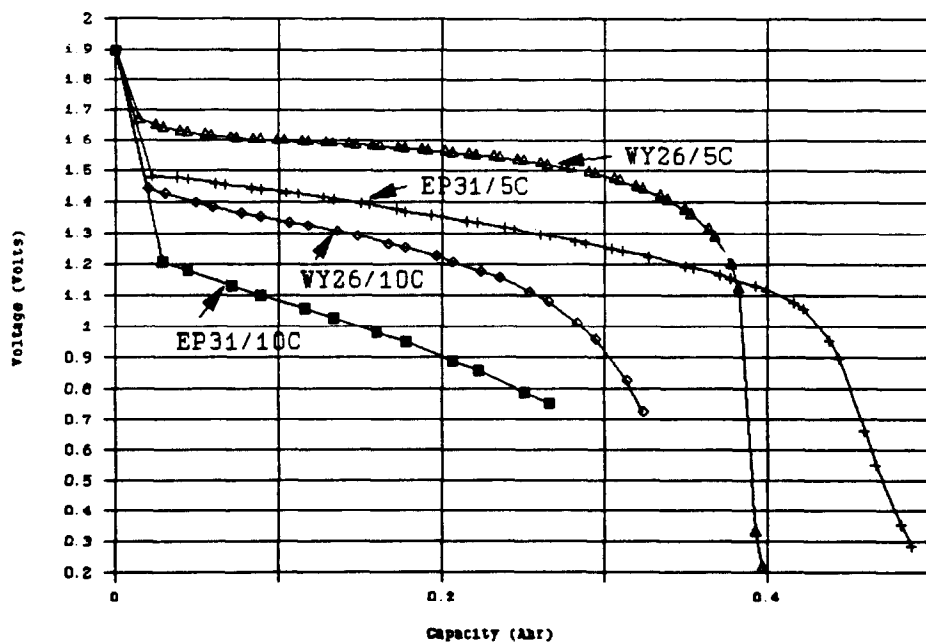

Fig. 4. 10 C and 5 C discharge voltage profiles *vs.* capacity during flooded electrode tests for Eagle Picher electrode in 31% KOH and Whittaker/Yardney electrode in 26% KOH.

TABLE 8

Capacities and A h efficiencies for flooded electrode tests

Discharge rate	Capacity (A h)		A h efficiency (%)	
	EP31	WY26	EP31	WY26
$C/4$	0.64	0.43	71.95	73.07
$C/2$	0.63	0.41	71.19	70.48
C	0.59	0.40	66.54	68.00
$2C$	0.55	0.39	61.92	67.43
$5C$	0.47	0.37	52.63	62.86
$10C$	0.25	0.33	28.20	56.90

the ability of the different electrodes to perform under actual battery conditions was not addressed. Thus, it is entirely possible that under actual battery conditions the Whittaker–Yardney electrodes would not perform optimally, and that the "starved" condition could lead to the type of poor performance that was seen at the high rates. Finally, it was not intended through these tests to compare the two manufacturers' electrodes directly. Neither manufacturer optimized the electrodes that were used; they simply supplied standard electrodes of the size requested.

Temperature variations between 0 °C and 30 °C produced some interesting results. As expected, an increase in temperature produced significant drops in EOC voltage due to the decrease in internal resistance that accompanies rising temperatures. Readings averaged 16.40 V at 0 °C and 15.12 V at 30 °C. As temperatures increased, the mid-point discharge voltages showed a steady increase at all discharge rates, except at $C/4$ where a 50 mV drop was seen between 0 °C and 10 °C (Table 7). The improved voltage performance seen at higher temperatures, however, did not directly translate into an increase in W h efficiencies at all conditions (Table 6). At the $2C$ rate discharge the W h efficiency was lowest (41.26%) at 30 °C and highest (53.43%) at 20 °C. At the other three discharge rates, though, 30 °C produced the highest efficiencies. The discrepancy at the $2C$ rate discharge can be, at least partially, attributed to a high EOD voltage of 10.3 V at 30 °C compared with 7.2 V at 20 °C. Whether or not the large percentage difference could have been completely overcome had the 30 °C discharge run down to around 7.0 V is difficult to determine, but, certainly, a large portion of it would have been. The effect that temperature had on total capacity out was equally interesting. For instance, as temperatures increased from 0 °C to 20 °C, capacity delivered to the normal cut-off points increased at the $C/2$ rate discharge from 41.19 A h to 47.68 A h, respectively, but fell off drastically at 30 °C to 37.50 A h (Table 4). This trend was consistent at all discharge rates and was also seen in the capacity data to the 10.0 V point in the discharge. Ampere hour efficiencies, however, seemed to be less consistently affected by temperature variations (Table 5). All these data seem to

support the use of temperatures as high as 20 °C, or even 30 °C, to produce optimum results. This agrees rather well with the data produced during the first battery test [1].

Increasing the H_2 pressure inside the vessel also produced some interesting results. Negligible change was seen in the EOC voltage between 200 and 400 psi as the voltage dropped from 15.62 V to 15.59 V, respectively; however, at 400 psi, an improvement was seen in the mid-point discharge voltage at all discharge rates (Table 7). This was expected behavior because the increased pressure would increase the activity coefficient of the gas and thus improve its efficiency and voltage performance. When looking at the data measured to the normal cut-off points in the discharge, the capacity, and A h and W h efficiencies, all were less at the higher pressure except at the $C/4$ rate discharge where a slight increase in both A h and W h efficiencies was seen (Tables 4 - 6). These were not expected results but, once again, the weak cell seems to be distorting the data by prematurely terminating the discharges during the 400 psi cycles. Although the capacity delivered to 10.0 V is still greater at 200 psi, the differences are not as great. Also, the A h and W h efficiency differences can be reasonably eliminated by considering the high EOD voltages on the 400 psi cycles. Actually, the W h efficiencies would have probably been greater at 400 psi had all discharges terminated at similar voltages. It certainly should illustrate that increasing or decreasing the pressure will have minimal effects on overall battery performance.

After completion of the characterization cycles, the battery was placed on LEO cycle life testing at 40% DOD and at 10 °C.

Conclusions and recommendations

Despite the fact that a weak cell made it difficult to compare directly some of the data from cycle to cycle, there was enough evidence to see that the battery produced generally expected results and performed very well throughout the majority of the characterization test matrix. It is hoped and expected that the LEO cycle life test that has just begun will produce similarly encouraging results. One area that continues to be a problem, however, is the high-rate discharge performance of the battery. Even though improvements were not made in this area with this battery, several encouraging ideas have been mentioned as possible solutions to the poor high-rate performance problem. As mentioned earlier, several studies, including small scale 2 in. × 2 in. battery tests, will be done in the hope of pinpointing the area or areas responsible for the poor high-rate performance.

References

1 R. L. Cataldo, Parametric and cycle tests of a 40 A h bipolar nickel–hydrogen battery, *21st Intersoc. Energy Conv. Eng. Conf., San Diego, CA, U.S.A., Aug. 25 - 29, 1986*, Vol. 3, American Chemical Society, Washington, DC, 1986, pp. 1547 - 1553.

2 H. S. Lim and S. A. Verzwyvelt, KOH concentration effect on the cycle life of nickel–hydrogen cells. II. Accelerated cycle life test, *21st Intersoc. Energy Conv. Eng. Conf., San Diego, CA, U.S.A., Aug. 25 - 29, 1986,* Vol. 3, American Chemical Society, Washington, DC, 1986, pp. 1601 - 1606.

3 H. Rogers, E. Levy, Jr., S. J. Stadnick, R. J. McGrath, H. S. Lim, T. L. Lisenbart and S. W. Darby, Failure mechanisms in nickel–hydrogen cells, final report, *Tech. Rep. AFAPL-TR-77-90,* Air Force Aero Propulsion Laboratory, Wright-Patterson Air Force Base, OH, December 1977, pp. 2 - 36.

4 R. L. Cataldo, Test results of a ten cell bipolar nickel–hydrogen battery, *18th Intersoc. Energy Conv. Eng. Conf., Orlando, FL, Aug. 21 - 26, 1983,* Vol. 4, American Institute Chemical Engineers, New York, 1983, pp. 1561 - 1567.